Opportunistic Conjunction Screening with Maneuvering Spacecraft

Max Geissbuhler, Joshua Horwood, Todd Brost, Navraj Singh, Jeff Aristoff

Slingshot Aerospace, 840 Apollo Street, Suite 100, El Segundo, CA 90245

ABSTRACT

In this paper, we present an innovative "opportunistic conjunction screening" approach that addresses conjunction assessment for on-orbit threats by considering the maneuvering capabilities of the conjuncting spacecraft and other factors such as lighting conditions and relative velocities. An example use case is when an adversarial spacecraft is actively thrusting, possibly to approach another spacecraft to perform imaging or some other nefarious action, and one would like to know which spacecrafts could be at risk over a particular screening window. We present two new algorithmic components used in the latest version of the software implementation of the opportunity screening approach. The first component is an enhancement to Slingshot's Implicit Runge-Kutta orbital propagator that permits the modeling of a continuous thrust acceleration that is sufficiently general to accommodate different types of thrusters such as chemical, ion, and electric. The second component is a new batch least squares estimator that jointly estimates an object's position-velocity state, drag and solar radiation pressure ballistic coefficients, and thrusting parameters given a sequence of observations from one or more optical sensors. We also show results from applying the new orbital state-thrusting parameter batch estimator using real data from the Slingshot Global Sensor Network on an active object in GEO.

1. INTRODUCTION

At AMOS 2016, we presented a novel approach to conjunction assessment (CA) screening and probability of collision (PC) calculation [1]. Like other conjunction analysis tools in existence today, the software implementation of this approach, called KRATOS (Kollision Risk Assessment Tool in Orbital element Spaces), originally only addressed **on-orbit hazards** (i.e., collisions with benign payloads or space debris). However, in the high-stakes space domain, additional considerations are needed to address **on-orbit threats**. First, one must consider the maneuvering capabilities of the conjuncting spacecraft. Second, one must consider other factors such as lighting conditions and relative velocities. It is thus necessary to screen for *opportunistic* conjunctions which we call "opportunistic conjunction screening," or more succinctly, "opportunity screening."

To address this need, Slingshot Aerospace has developed an innovative opportunity screening tool in the form of a web application that is used to provide key insights to its space operations customers. Specifically, the opportunity screening tool performs an "all-vs-all" CA screening using KRATOS where the "all" comprises all active payloads. A higher-than-normal miss distance threshold than what would normally be used in a traditional CA run is used to find all possible screening opportunities (e.g., a primary that may attempt to image a secondary). Conjunctions are further filtered to include only those that favor screening opportunities (e.g., a low relative velocity at the time-of-closest approach and favorable lighting conditions inferred from solar and lunar phase angles). The web app presents those screening opportunities to the analyst in the form of a sortable and filterable table. The user may select a particular conjunction and choose to examine additional metrics and graphics on the details of the screening opportunity.

Importantly, the opportunity screening tool also accounts for possible maneuver plans and thrusting capabilities of any of the active payloads used in the CA. In other words, the prediction of orbital states used in the CA assumes not only nominal motion (gravity, third-body perturbations, atmospheric drag, solar radiation pressure, etc.), but also permits maneuver plans and estimated or prescribed thrusting capabilities in the orbital predictions. An example use case is when an adversarial spacecraft is actively thrusting, possibly to approach another spacecraft to perform imaging or some other nefarious action, and one would like to know which spacecrafts could be at risk over a particular screening window.

In this paper, we present two main algorithmic components that are used in the latest version of the opportunity screening web app that account for maneuvering spacecraft and support the aforementioned use case.

The first component is an enhancement to Slingshot's Implicit Runge-Kutta orbital propagator (IRKProp) [2, 3] that permits the modeling of a continuous thrust acceleration (parameterized in terms of the thrusting start and end times, total velocity increment (Delta-v) magnitude, propellant exhaust velocity magnitude, and thrusting direction vector) that is sufficiently general to accommodate different types of thrusters such as chemical, ion, and electric. The second component is a new batch least squares estimator that jointly estimates an object's position-velocity state, drag and solar radiation pressure (SRP) ballistic coefficients (BCs), and thrusting parameters given a sequence of angle-only observations from one or more optical sensors.

Besides presenting the underlying optimization problem for joint orbital state and maneuver estimation, we demonstrate that its solution is feasible and accurate for several reasons. First, we can "hot start" the iterative non-linear least squares procedure using an approximate orbital state and maneuver alert generated from Slingshot's Multiple Frame Assignment Space Tracker (MFAST) software [4]. Second, we can obtain sufficient data needed to estimate all orbital state components and thrusting parameters from sensors in the Slingshot Global Sensor Network (SGSN) [5], even when a spacecraft is actively thrusting. We also show results from applying the new orbital state-thrusting parameter batch estimator using real SGSN data on active payloads. Ultimately, we demonstrate that once an accurate orbital state is estimated with thrusting parameters, one can accurately propagate the orbit and assess screening opportunities against other objects via KRATOS, which has been upgraded to ingest maneuver plans.

The plan of the paper is as follows. In Section 2, we outline the technical approach beginning with an overview of the opportunity screening web app followed by a description of some of the key algorithmic components and recent improvements made to them, including IRKProp, the joint orbit-thrust parameter batch least squares estimator, and KRATOS. In Section 3, we demonstrate the web app using data from the SGSN, where the primary thrusting object is AMC-6 (NORAD ID 26580). In Section 4, we present conclusions.

2. TECHNICAL APPROACH

The opportunistic conjunction screening web app comprises three main components which we briefly describe below.

1. **Joint Orbit and Thrust Parameter Estimation.** Given a sequence of angle-only observations on a single primary object, a batch least squares problem is solved for the primary's position-velocity state, drag and SRP BCs, and thrust parameters (see Section 2.2 for additional details). The latter comprise the parameters of a single continuous thrust in terms of the thrust start and end times, Delta-v magnitude, and thrusting direction vector (see Section 2.1 for additional details). The user can configure the fit span, maximum number of tracks to use over the fit span (for runtime considerations), and a starting guess for the thrust duration. The output includes a residuals plot, the estimated orbital and thrust parameters, and diagnostic log messages. The latter notifies the user if (i) no thrusting was detected within the fit span; (ii) thrusting was detected but ended prior to the new epoch time (the time of the last track); or (iii) thrusting is active (i.e., the object is still thrusting at the new epoch time). The user may choose to rerun the batch with different parameters or choose to accept the results. The latter triggers a one-vs-all CA run.

2. **One-vs-All Conjunction Assessment.** Using the state estimate and any thrust parameters obtained from the procedure above, a CA screening is performed on this "one" primary object against all active payloads using KRATOS (see Section 2.3). If the primary object is actively thrusting, it is hypothesized to be thrusting over the entire screening interval with the same thrust acceleration vector estimated in the batch least squares procedure. To capture imaging and screening opportunities, a miss distance threshold of 250 km is used (which is much higher than what would normally be used in traditional CA). The web app presents those screening opportunities to the user in the form of a sortable table. The user may select a particular conjunction and choose to examine additional graphics and visualizations on the details of the screening opportunity.

3. **Conjunction Visualization.** Once the user selects a conjunction to review, the web app displays several plots that show the time evolution of various quantities over the screening interval. These include the

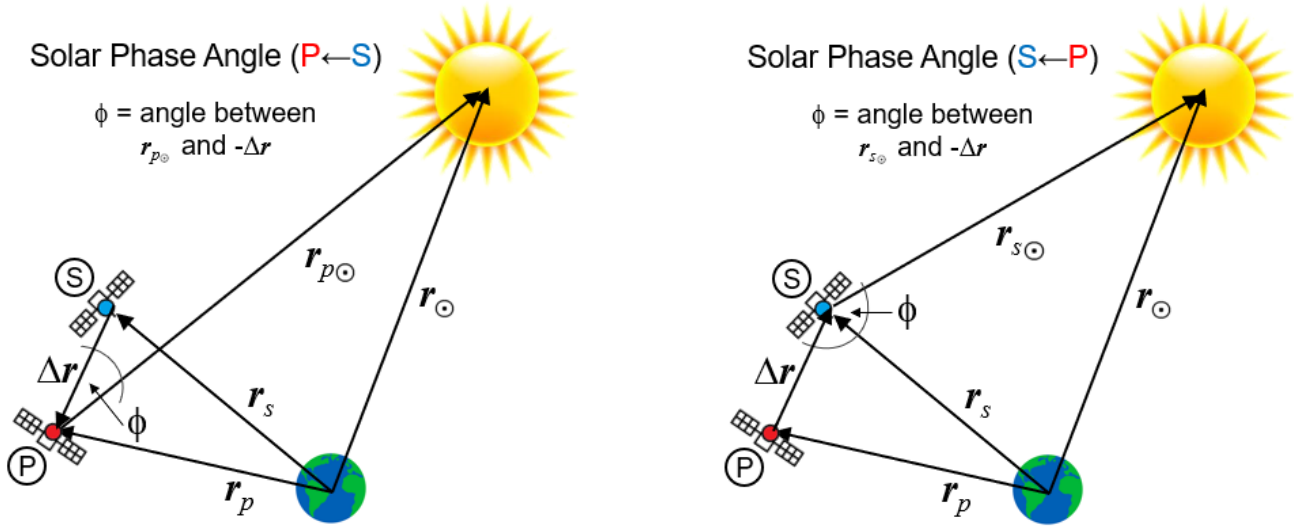

(a) Primary solar phase angle relative to secondary (b) Secondary solar phase angle relative to primary

Figure 1. Definitions of Relative Solar Phase Angles

relative position (and components along the radial, in-track, and cross-track directions), relative velocity, angular rate, and solar and lunar phase angles of the primary relative to the secondary and of the secondary relative to the primary. Definitions of the relative solar phase angles are shown in Figure 1; the relative lunar phase angles are defined similarly. Generally, if a primary object is seeking to image a secondary, one would require these phase angles to be less than 90°. The web app also displays "timeline" plots that show when the range, relative speed, angular rate, and phase angles are each below their respective thresholds that favor imaging opportunities.

Usage of the opportunity screening web app is usually not a "one and done" procedure especially if the primary object is actively thrusting. In such cases, the user will typically request additional tracking data on the thrusting object. Once new observations are received, the user can rerun the web app (using the latest data) to assess how the conjunctions of interest have evolved.

In what follows, we discuss some of the algorithmic and feature enhancements made to IRKProp, the batch least squares estimator, and KRATOS that have facilitated the development of the opportunity screening web app.

2.1 Implicit Runge-Kutta Orbital Propagator (IRKProp)

Slingshot's IRKProp is the primary orbital propagator used in Slingshot's KRATOS and MFAST software, in various web applications that require orbital predictions such as opportunity screening, and elsewhere in the SGSN pipeline. The numerical integration method within IRKProp is A-stable (it can be applied to problems with multiple time scales), super-convergent (it achieves the highest order of convergence possible by using Legendre polynomials as the interpolating basis within the implicit Runge-Kutta scheme), and adaptive (because it estimates and controls the error by automatically adjusting the step size) [2, 3]. Dynamics modelled in the propagator include (i) gravity using the EGM-2008 spherical harmonic model; (ii) solar and lunar third-body perturbations; (iii) atmospheric drag using the NASA Jacchia-70 atmosphere model; (iv) solar radiation pressure based on a "cannonball" model with an Earth-Sun umbra/penumbra shadow model; and (v) optional continuous thrusting. The latter is a recent upgrade to IRKProp to support Slingshot's R&D in maneuver and change detection algorithms and development of the opportunity screening web app.

In particular, the continuous thrust model in IRKProp makes the following assumptions:

1. The force due to thrust is constant over a given time interval $[t_0, t_0 + \Delta t]$.

2. The spacecraft has a fixed propellant mass flow rate $|\dot{m}|$ such that its mass at time t is described by $m(t) = m_0 - |\dot{m}|(t - t_0)$, where m_0 is the mass at the start time t_0 of the burn.

3. The mass expended over the burn is negligible compared to the starting mass of the spacecraft. In other words, $|\dot{m}|\Delta t \ll m_0$.

The resulting acceleration model for a thrusting spacecraft uses the following input parameters:

i. start time, t_0
ii. burn duration, Δt
iii. total velocity increment magnitude, Δv
iv. exhaust velocity magnitude, v_e
v. thrust direction (unit vector) with respect to the RIC frame, $\boldsymbol{u}$

The model is sufficiently general since different thrust systems will have different values of the parameters above (see, for example, Table 3.1.3 in [6]). The implementation of this acceleration in IRKProp also allows one to specify multiple thrusts over the integration interval via multiple sets of the parameters (i)–(v) above.

2.2 Joint Orbit and Thrust Parameter Estimation

In the general non-linear estimation problem, one is given a sequence of N reports $\boldsymbol{Z}_N = \{\boldsymbol{z}_k\}_{k=1}^N$ (e.g., sensor observations, tracks) with respective time-tags $\{t_k\}_{k=1}^N$. The objective of the estimation problem is to obtain a representation of the joint posterior probability density function (PDF) $p(\boldsymbol{y}_0, \ldots, \boldsymbol{y}_N | \boldsymbol{Z}_N)$ or the marginal PDF $p(\boldsymbol{y}_N | \boldsymbol{Z}_N)$, where $\boldsymbol{y}_k$ denotes the system state at time t_k, subject to dynamical and measurement models. This problem can be solved by either processing all reports simultaneously through a batch process (e.g., non-linear least squares) or sequentially through a non-linear filter (e.g., Kalman filter).

For the joint orbit and thrust parameter estimator used in the opportunity screening web app, the state vector $\boldsymbol{y}_k$ is decomposed as $(\boldsymbol{x}_k, \boldsymbol{\alpha}_k)$, where $\boldsymbol{x}_k$ is the inertial position-velocity (PV) vector (with respect to the MEME-J2000 frame) and $\boldsymbol{\alpha}_k$ is a vector that includes the thrust parameters, drag BC (only for near-Earth objects), and SRP BC. For the latter, we assume $\boldsymbol{\alpha}_k = \boldsymbol{\alpha}_{k-1} \equiv \boldsymbol{\alpha}$; i.e., the thrust parameters and BCs are constant over the fit span. Further, as detailed in Section 2.1, we set

$$\boldsymbol{\alpha} = (t_0, \Delta t, \Delta v, \boldsymbol{u}, \beta_{drag}, \beta_{srp}),$$

where t_0 is the start time of the thrust, Δt is the duration of the thrusting, Δv is the total velocity increment magnitude, $\boldsymbol{u}$ is the thrusting direction with respect to the RIC frame, β_{drag} is the drag BC, and β_{srp} is the SRP BC. One could accommodate a more general thrust parameter vector $\boldsymbol{\alpha}$, such as one that includes multiple thrusting intervals or includes the exhaust velocity magnitude. The latter is a higher-order term in the thrust acceleration and can be numerically unobservable. We omit v_e in the estimation (or effectively let $v_e \to \infty$).

Appealing to Bayes' rule, the joint PDF in $\boldsymbol{y}_N = (\boldsymbol{x}_N, \boldsymbol{\alpha})$ conditioned on the measurement sequence $\boldsymbol{Z}_N$ can be derived (see, for example, Jazwinski [7, §5.3]). The non-linear least squares (NLLS) problem results from maximizing this joint PDF or, equivalently, minimizing the negative logarithm of the joint PDF.

Methods for solving NLLS problems, such as Gauss-Newton, full Newton, and quasi-Newton updates, along with globalization methods such as line search and trust region methods including Levenberg-Marquardt [8], are efficient and mature, and we will not elaborate on them further.

Often the most challenging step of solving a NLLS problem such as the one discussed here involves defining the starting iterate or "guess". Within the SGSN pipeline, we obtain a starting guess for the PV state $\boldsymbol{x}_N$ by querying the SGSN catalog for the latest (possibly pre-maneuver) state on the object and propagate it to time t_N using IRKProp with a nominal motion model. Proposing a starting guess for the thrust parameters is more challenging. Active objects in the SGSN catalog are maintained with an interacting multiple model filter [9] with a "low" and "high" process noise model, where the latter is tuned to capture maneuvers. When the filter transitions from the low to high process noise model, a maneuver alert gets generated. The time-tag of the

alert along with the filtered states from the low and high models can be used to obtain a crude estimate of the thrusting start time, Delta-v magnitude, and thrusting direction.

Another important consideration is the observability of the state vector $\boldsymbol{y}_N$. Loosely speaking, we seek to know what components of $\boldsymbol{y}_N$ (or linear combinations of such components) can be "estimated". Such an assessment can be revealed from a singular value decomposition (SVD) of the Jacobian matrix of the NLLS residual vector. An example of this observability analysis via the SVD for the NLLS problem that arises in sensor calibration is described in Herman and Poore [10]. For the NLLS problem under consideration, we sometimes see that the thrusting start or end times are unobservable. The diagnostic log messages that are shown in the web app display warnings on any potentially unobservable parameters. For example, if the thrusting end time is unobservable, it suggests that the object may be actively thrusting.

2.3 Kollision Risk Assessment Tool in Orbital element Spaces (KRATOS)

Slingshot's KRATOS software suite performs rapid CA screening and generates more accurate PCs to reduce false alarms and misdetections. The first version of KRATOS was presented at AMOS 2016 [1]. Since then, a number of algorithmic improvements and feature enhancements have been made to KRATOS, in particular, ones that support the opportunity screening web app. We describe the salient features of the present version of KRATOS below.

As primary inputs, KRATOS accepts the Vector Covariance Message (VCM) or Conjunction Data Message (CDM). Optionally, an owner/operator (O/O) ephemeris can be provided for one or more object IDs. In such a case, the ephemeris data is used in the CA and PC algorithms instead of KRATOS generating the ephemeris itself using Slingshot's IRKProp. If provided, any O/O ephemeris must be in the modified ITC format (as described in the 18 SDS Spaceflight Safety Handbook [11]). The O/O ephemeris can include maneuver plans and launch plans embedded within the trajectory. This input format is used for the primary object in the opportunity screening web app.

KRATOS CA enables one-vs-one, one-vs-all, all-vs-all, some-vs-some, and some-vs-all screening scenarios, all of which are computationally viable on catalogs with 100k objects or more using efficient multi-core processing. KRATOS CA can also report multiple conjunctions over a given screening interval. Conjunction assessment filtering uses algorithms from the European Space Agency (ESA) smart sieve filters [12, 13] which quickly and cheaply identify potential conjunction risks.

KRATOS PC leverages multiple PC algorithms, both traditional (NASA/Foster, Coppola, Monte-Carlo) and Slingshot-developed (Gaussian sums), and it includes an adaptive methodology to automatically select the PC method based on what assumptions are met, so that more computationally expensive techniques are used only when needed. To provide superior covariance realism, KRATOS represents states and covariances in equinoctial orbital elements (since this coordinate system allows Gaussian assumptions to be preserved more closely under the non-linear dynamics than Cartesian coordinates). In extreme cases where it may not be possible to describe the orbital uncertainty by a single Gaussian covariance (in equinoctial space), the KRATOS PC Gaussian sum method provides a robust methodology to compute the PC in such non-linear and non-Gaussian regimes which rivals the accuracy of Monte-Carlo methods but at significantly less computational expense.

The KRATOS algorithms have been hardened and validated on a wide range of relevant datasets including benchmark test cases published by Alfano [14] and real VCM data of the public catalog from April of 2015 courtesy of 18 SDS (comprising ∼16,000 objects). KRATOS runs as a "cron job" to regularly process SGSN state vectors (and covariances) and outputs conjunction alert messages.

3. RESULTS AND DISCUSSION

We now demonstrate the opportunity screening web app on a real example that was run on AMC-6 (NORAD ID 26580) at approximately 2022-08-11T14:30:00Z. This case was motivated by a maneuver alert that was triggered on this object earlier in the day. Figure 2 shows a screenshot of the web app where the user can configure the various parameters for the joint orbit and thrust parameter estimation. In this example, we selected a fit span of 3 days asking to use at most 100 SGSN tracks, a thrust duration guess of 600 s, and made requests to estimate both the start and end thrusting times.

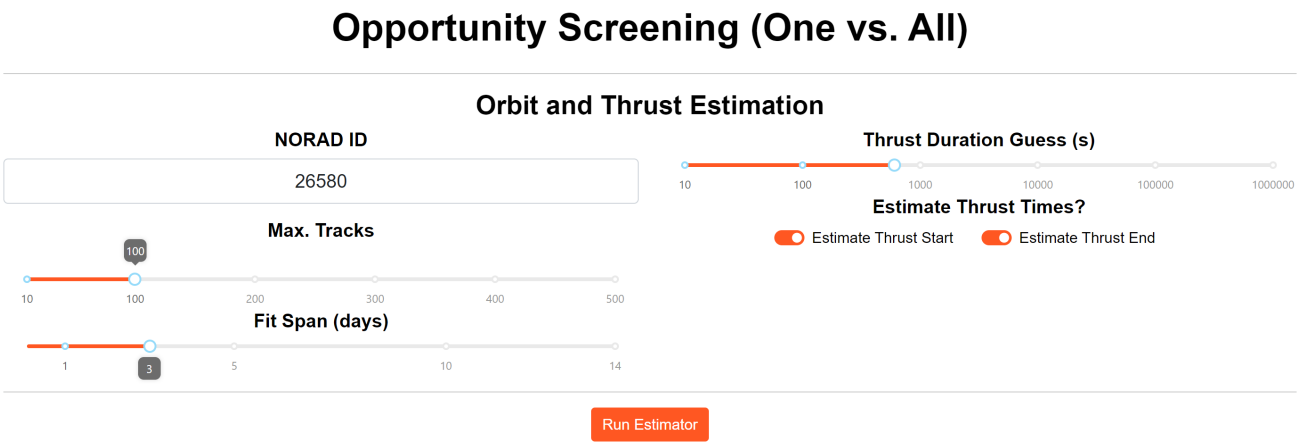

Figure 2. AMC-6 Opportunity Screening Example: Initial Parameter Selections

Upon selecting the "Run Estimator" button, the joint orbit and thrust parameter estimator was invoked. The log messages stated that 92 tracks were found over the fit span, thrusting was detected, the resulting weighted RMS from the batch fit was 1.3, and no thrusting parameters were found to be unobservable. Figure 3 shows a screenshot of the web app that displays the estimated orbital and thrust parameters. In particular, we see that the Delta-v estimate of 1.310 m/s is quite certain with only an (one-sigma standard deviation) uncertainty of 0.01 m/s. The start and end thrusting times are certain to within about 11 and 14 minutes, respectively, and the thrusting direction is predominantly along the positive cross-track direction (which suggests an inclination raising maneuver).

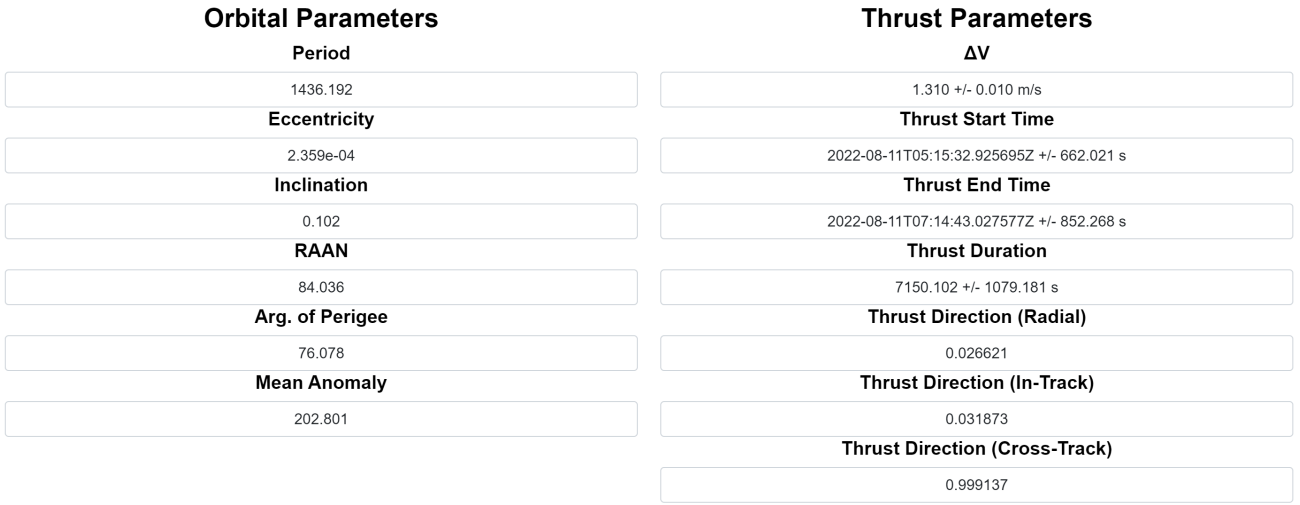

Figure 3. AMC-6 Opportunity Screening Example: Estimated Orbital and Thrust Parameters

Figure 4 shows the measurement residuals against the batch-fitted orbit. In order to show both the angle and angle-rate measurement residuals on a common plot, we display the residuals as normalized Gaussian z-scores (i.e., the absolute residual divided by the corresponding sensor measurement standard deviation). For a good fit, we expect to see most of the residuals within plus or minus three standard deviations (i.e., about 99.7% of the total probability of the standardized Gaussian PDF), apart from an occasional outlier, which is what we see in this example.

By analyzing the log messages, estimated orbit and thrust parameters, and measurement residuals plot, the user can choose to accept the batch fit by selecting the "Run KRATOS" button. In this example, this invokes a KRATOS CA run of AMC-6 against all other active payloads over a one-day screening interval starting from

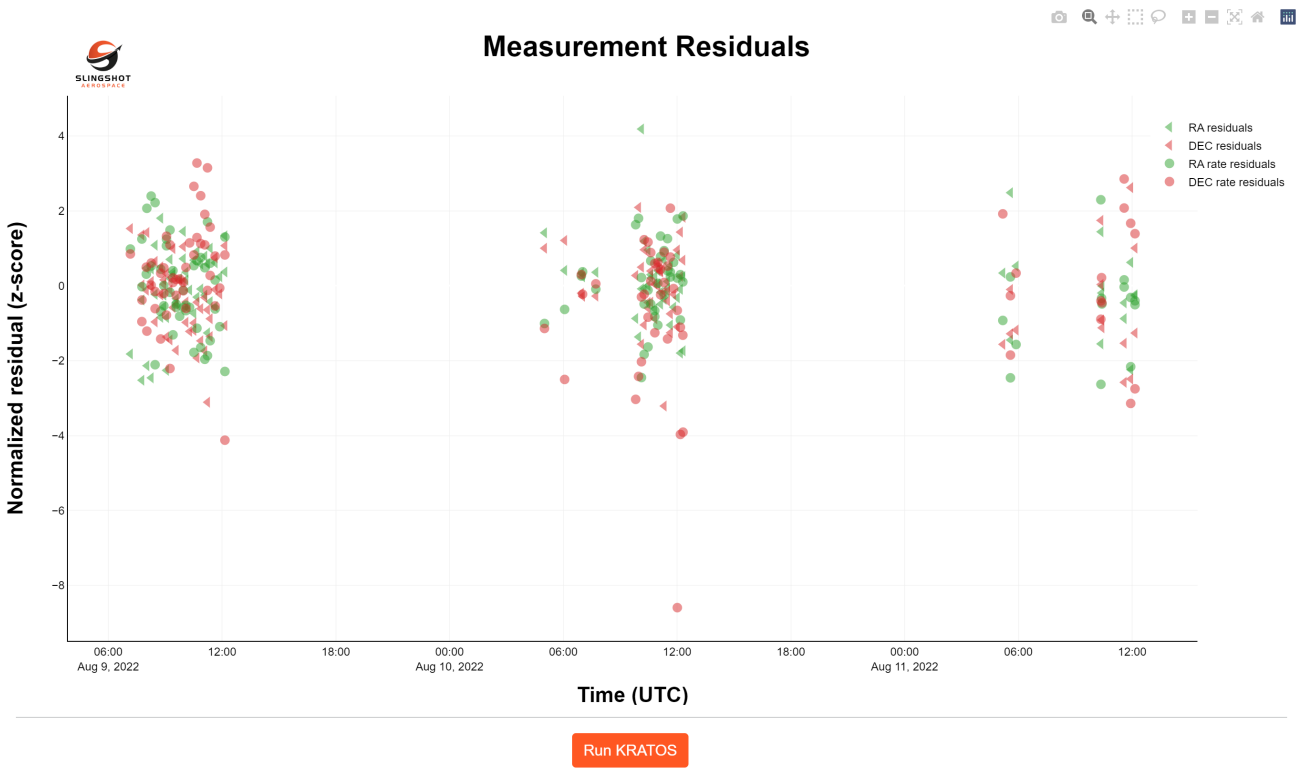

Figure 4. AMC-6 Opportunity Screening Example: Measurement Residuals

the time the "Run KRATOS" button is selected. Figure 5 shows the results of this conjunction analysis. Three conjunctions were found with miss distances less than 250 km. For each conjunction, the table shows traditional CA metrics including the miss distance, time of closest approach (TOCA), and the relative speed and angular rate at the TOCA. For each of the primary and secondary objects, the table shows the NORAD ID, common name, country of origin, whether the object is illuminated by the Sun, and the solar and lunar phase angles. We see that all three conjunctions have low relative velocities and angular rates at the TOCA and could present favorable imaging opportunities.

	Conjunction				Primary						Secondary					
	MD (km)	Speed (km/s)	Ang. Rate (deg/s)	TOCA	NORAD ID	Name	Country	Illuminated	Solar PA (deg)	Lunar PA (deg)	NORAD ID	Name	Country	Illuminated	Solar PA (deg)	Lunar PA (deg)
○	205.997	0.773	0.215	2022-08-12T00:17:42.627Z	26580	AMC-6 (GE-6)	SES	Y	25.3	148.8	23880	GORIZONT 32	CIS	Y	154.7	31.2
◉	57.054	0.112	0.112	2022-08-12T05:44:20.017Z	26580	AMC-6 (GE-6)	SES	Y	135.5	36.9	28903	SPACEWAY 2	US	Y	44.5	143.1
○	146.106	0.123	0.048	2022-08-12T05:46:14.354Z	26580	AMC-6 (GE-6)	SES	Y	41	146.5	28187	EUTE 7A (EUTE W3A)	EUTE	Y	139	33.5

Inspect Conjunction

Figure 5. AMC-6 Opportunity Screening Example: Table of Conjunctions

In this AMC-6 example, we selected the conjunction with SPACEWAY 2 (NORAD ID 28903) and selected the "Inspect Conjunction" button to generate a series of plots. Note that in all plots, the primary is AMC-6 and the secondary is SPACEWAY 2. Figure 6 shows the timeline plots for the primary relative to the secondary (P ← S) and the secondary relative to the primary (S ← P) over the one-day screening interval. The plots show when the range, relative speed, angular rate, and phase angles are each below their respective thresholds that favor imaging opportunities. Said thresholds are given below:

- Range: Less than 250 km
- Relative speed: Less than 2 km/s

- Angular rate: Less than 3°/s
- Phase angle: Less than 90°

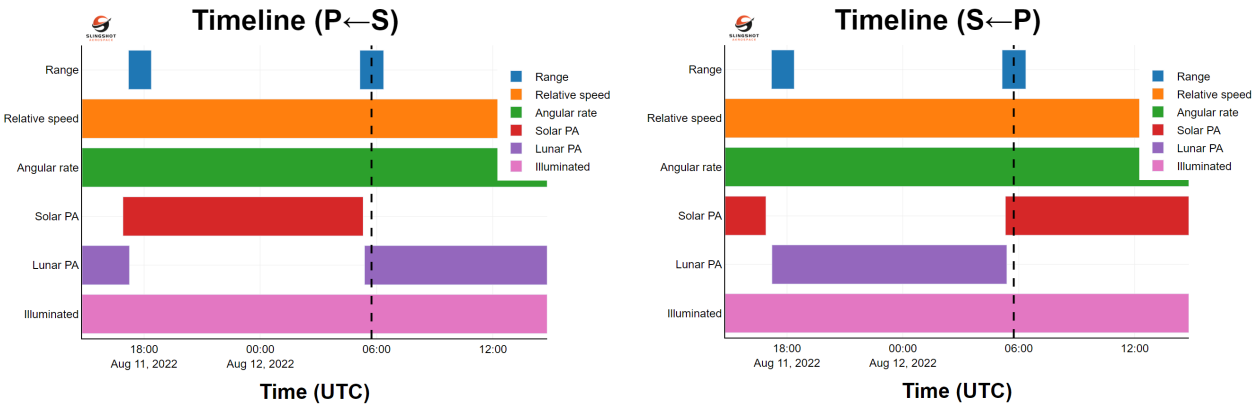

Figure 6. AMC-6 Opportunity Screening Example: Timeline for Favorable Imaging Opportunities

Examining the S ← P timeline plot on the right, we see that all metrics except for the lunar phase angle are below their respective thresholds at the TOCA (indicated by the vertical dashed line). Thus, the opportunity for AMC-6 to image SPACEWAY 2 at the TOCA could be considered favorable but not perfect because the lunar phase angle is 143.1° (recall the definition of these phase angles in Figure 1).

Figure 7 shows the evolution of the range (broken down into radial, in-track, and cross-track components) and phase angles for this AMC-6 (primary) and SPACEWAY 2 (secondary) example. We see that the cross-track component of the relative position changes the most over the screening interval. The phase angles change most rapidly around the conjunction times.

Figure 8 shows the evolution of the relative speed and angular rate. We see that both rates are very small over the entire one-day screening interval (consistent with the timeline plots in Figure 6) suggesting that AMC-6 may be slowly drifting towards SPACEWAY 2 (additional analysis not provided in the web app reveals that the difference in drift rates is quite small and the closure rate is very slow).

In closing, we remark that the opportunity screening web app is applicable to *all* regimes of space, including LEO, and Slingshot has used the web app to assess conjunctions of active objects in LEO (and GEO, as this example illustrated).

4. CONCLUSIONS

In this paper, we demonstrated how one can take traditional CA for on-orbit hazards to the next level by addressing on-orbit threats involving actively maneuvering spacecraft. We presented a newly developed web application that performs CA on a payload, that could be actively thrusting, against all other active payloads, and provides the ability to screen the conjunctions for favorable imaging opportunities. We also described some of the key algorithmic components that drives the web app under the hood including the Slingshot IRKProp that now permits modeling of a continuous thrust acceleration, a new joint orbit-thrust parameter estimator, and advancements to Slingshot's KRATOS CA/PC software. We demonstrated the web app on live Slingshot Global Sensor Network data from AMC-6 which had just conducted an inclination raising maneuver and was about to come in close proximity to three other active payloads within the next day. The new opportunistic conjunction screening web app effectively provides a tool to assess if an adversarial spacecraft is actively thrusting possibly to approach another spacecraft to perform imaging or some other nefarious action. The tool also estimates the parameters of the thrusting, identifies spacecrafts the adversary could reach, and provides metrics and visualizations of any resulting conjunctions.

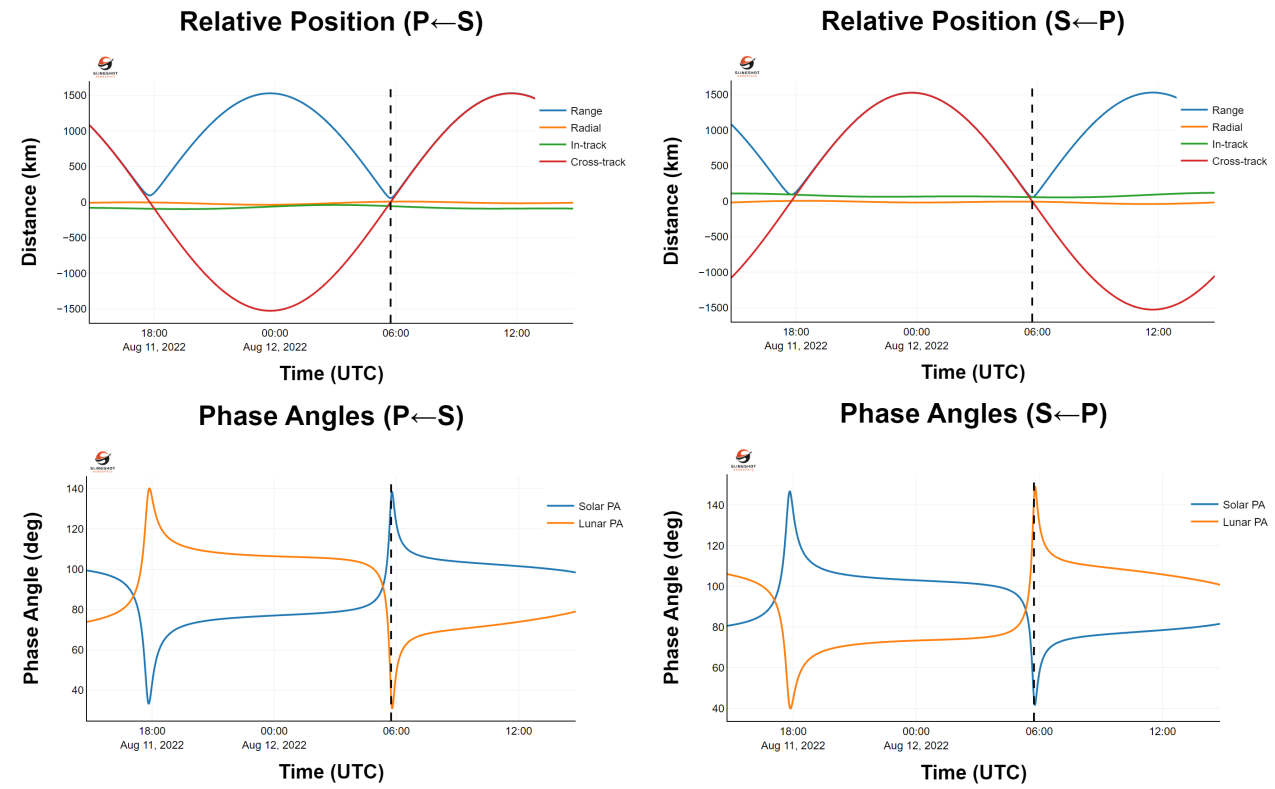

Figure 7. AMC-6 Opportunity Screening Example: Evolution of Range and Phase Angles

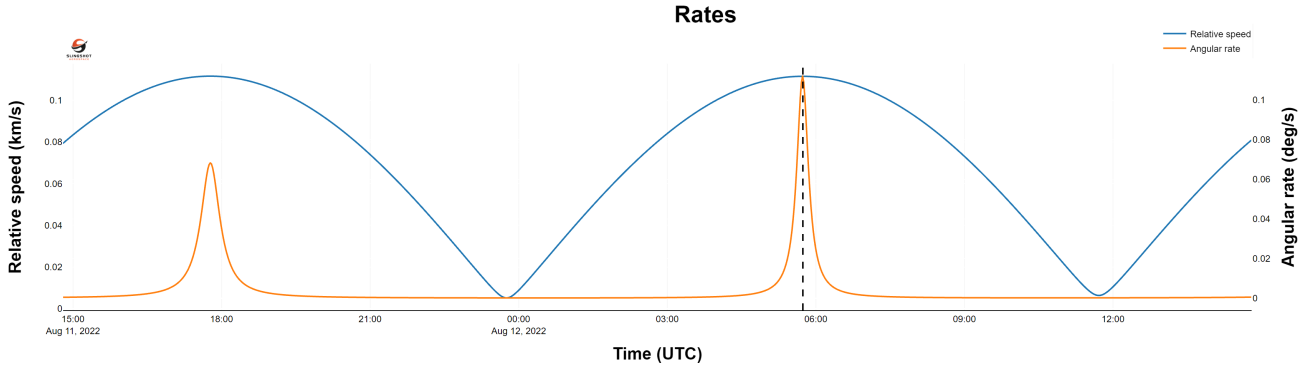

Figure 8. AMC-6 Opportunity Screening Example: Evolution of Relative Speed and Angular Rate

REFERENCES

[1] J. T. Horwood, N. Singh, J. M. Aristoff, and A. Bhopale, "KRATOS: Kollision Risk Assessment Tool in Orbital Element Spaces," in *Proceedings of the 2016 Advanced Maui Optical and Space Surveillance Technologies Conference*, (Wailea, HI), September 2016.

[2] J. M. Aristoff, J. T. Horwood, and A. B. Poore, "Orbit and uncertainty propagation: a comparison of Gauss-Legendre-, Dormand-Prince-, and Chebyshev-Picard-based approaches," *Celestial Mechanics and Dynamical Astronomy*, vol. 117, pp. 13–28, 2013.

[3] J. M. Aristoff, J. T. Horwood, and A. B. Poore, "Implicit Runge-Kutta-based methods for fast, precise, and scalable uncertainty propagation," *Celestial Mechanics and Dynamical Astronomy*, vol. 122, no. 2, pp. 169–182, 2015.

[4] J. M. Aristoff, D. J. C. Beach, P. A. Ferris, J. T. Horwood, A. D. Mont, N. Singh, and A. B. Poore,

"Multiple Frame Assignment Space Tracker (MFAST): results on UCT processing," in *Proceedings of the 2015 AIAA/AAS Astrodynamics Specialist Conference*, (Vail, CO), August 2015. Paper AAS 15-675.

[5] J. Aristoff, A. Ferris, A. Larson, N. Singh, J. Horwood, J. Shaddix, K. Wilson, T. Lyons, and N. Dhingra, "Non-traditional data collection and exploitation for improved GEO SSA via a global network of heterogeneous sensors," in *Proceedings of the 2018 Advanced Maui Optical and Space Surveillance Technologies Conference*, (Wailea, HI), September 2018.

[6] O. Montenbruck and E. Gill, *Satellite Orbits: Models, Methods, and Applications*. Berlin: Springer, 2000.

[7] A. H. Jazwinski, *Stochastic Processes and Filtering Theory*. New York: Dover, 1970.

[8] R. Fletcher, *Practical Methods of Optimization*. Chichester: John Wiley & Sons, 1991.

[9] Y. Bar-Shalom, X.-R. Li, and T. Kirubarajan, *Estimation with Applications to Tracking and Navigation*. New York: John Wiley & Sons, 2001.

[10] S. M. Herman and A. B. Poore, "Nonlinear least-squares estimation for sensor and navigation biases," in *SPIE Proceedings: Signal and Data Processing of Small Targets 2006*, vol. 6236, 2006.

[11] 18th Space Defense Squadron, "Spaceflight safety handbook for satellite operators," tech. rep., August 2020.

[12] J. R. Alarcón-Rodríguez, F. M. Martínez-Fadrique, and H. Klinkrad, "Collision risk assessment with a 'smart sieve' method," in *Proceedings of Joint ESA-NASA Space-Flight Safety Conference*, (Noordwijk, Netherlands), pp. 159–164, June 2002.

[13] J. R. Alarcón-Rodríguez, F. M. Martínez-Fadrique, and H. Klinkrad, "Development of a collision risk assessment tool," *Advances in Space Research*, vol. 34, pp. 1120–1124, 2004.

[14] S. Alfano, "Satellite conjunction Monte Carlo analysis," in *Proceedings of the 19th AAS/AIAA Space Flight Mechanics Meeting*, (Savannah, GA), February 2009. Paper AAS-09-233.